Nonlinear Control of Hybrid Drones via Optimised Control Allocation

Gil Serrano[1], Bruno Guerreiro[1,2], and Rita Cunha[1]

[1] Institute For Systems and Robotics (ISR/LARSYS), Instituto Superior Técnico, 1049-001, Lisbon, Portugal
[2] DEEC and CTS/UNINOVA, NOVA School of Science and Technology, 2829-516 Caparica, Portugall
E-mails: gil.serrano@tecnico.ulisboa.pt, bj.guerreiro@fct.unl.pt, and rita@isr.tecnico.ulisboa.pt

Abstract. This work addresses the development of a unified control strategy, based on nonlinear control techniques, for hybrid tri-tiltrotor UAVs, so that a simple trajectory is followed. A model of a tri-tiltrotor UAV is derived, detailing the forces and moments that act on the system, followed by a unified control approach that considers the system dynamics as a whole. Backstepping control and nonlinear optimisation are used for position and attitude control to calculate force and moment references and a control allocation strategy based on nonlinear optimisation is proposed. Two trajectories are defined; in the first trajectory, the UAV is expected to fully transition from rotary-wing to fixed-wing configuration, while in the second, it is expected to fly in an intermediate configuration. To validate the approach, simulations for these trajectories are performed and the results are analysed.

Keywords: Hybrid UAV, Tiltrotor UAV, Backstepping control, Control Allocation, Trajectory tracking

1 Introduction

The usage of UAVs has grown considerably over the past years as more applications are found for these vehicles. Depending on the nature of the application, the type of UAV that has the best performance for a certain task may vary. Fixed-wing and rotary-wing UAVs are ubiquitous. Despite their predominance, both types of UAV present a distinct set of advantages and disadvantages. Hybrid UAVs attempt to mitigate the shortcomings and combine the strengths of both types of aircraft. These UAVs are typically fixed-wing vehicles with VTOL capabilities, which are more effective in a wider range of scenarios, due to the ability to fly at high speeds, with a long flight range and greater payload capacity, with the possibility to vertically take off and land without a runway.

This work, which was developed within the scope of the REPLACE project [1], addresses the design of nonlinear control techniques for trajectory tracking with hybrid tiltrotor UAVs. The usual control approach for hybrid vehicles is to employ hybrid control techniques, defining several modes of operation that are

less complex than the entire system, developing controllers for each mode, and switching between them. In the case of hybrid UAV, a common approach is to consider a rotary-wing and a fixed-wing mode. One of the objectives of this work is to take the initial steps towards a unified control approach to tiltrotor UAVs, considering the system as a whole, instead of having different modes of operation. Another goal is to have the UAV fly in an intermediate configuration, neither fully in rotary-wing nor in fixed-wing mode. To achieve this, a trajectory that takes the aircraft up to a certain altitude and then begins flying forward will be devised. Next, taking into account a dynamic model of the UAV, the unified nonlinear control strategy will be derived and tested in simulation.

The remainder of this work is organised as follows. Section 2 provides a brief overview of research on hybrid UAVs. Section 3 describes the nonlinear model of a tri-tilrotor UAV. Section 4 delineates the unified control approach, using backstepping to control the position and attitude of the UAV, as well as the control allocation scheme, based on nonlinear optimisation. Section 5 describes the reference trajectories and presents the simulation results and the evaluation of the performance. Finally, Section 6 summarises the work developed.

2 Related Work

The past decade has seen an increase in research work on hybrid UAV. Much work is focused on developing control algorithms that target one of the operation modes of these vehicles, while others opt for a more comprehensive approach to the problem, usually resorting to hybrid control techniques.

Regarding hybrid control of tri-tiltrotor UAVs, in [2], the dynamical model of the aircraft is divided into two: in hover mode, in which aerodynamic effects are neglected, and in cruise flight mode, with a simplified model of these effects. The control strategy takes into account the longitudinal dynamics for altitude and attitude control, i.e. only pitch motion is stabilised by a PID controller, with roll and yaw controlled manually and the defined trajectory has a trapezoidal velocity profile. The modelling and control of a tri-tiltrotor UAV is also the subject of [3], though only for hover mode. An attitude PID controller and a control allocation scheme based on the desired roll and pitch moments and (vertical) thrust are designed, tested in simulation and experimentally with adequate results in altitude stability, despite a more oscillatory behaviour in terms of attitude control. A more complete nonlinear model of a tri-tiltrotor UAV is derived in [4], with emphasis on transition dynamics, studied in computational fluid dynamics simulations. A hybrid approach that switches between hover, transition and cruise flight controllers is implemented, though simulation results show that the UAV's altitude decreases with every controller switch.

Unified approaches to control of hybrid UAV, though less common than hybrid approaches, have also been developed. In [5], the flight envelope of a tiltwing UAV is studied and modelled via wind tunnel tests, defining a continuous flight configuration space that contains the different flight modes, thus not needing to define discrete flight configurations. With this strategy, a map-based feedforward

controller independent of the flight state for motion control is developed. The tilt angle of the wing is obtained in conjunction with the aircraft's pitch angle dependent on the flight state. The approach in [6], for a quad-tailsitter UAV, handles the flight modes continuously as well. In this case, the aircraft's attitude changes significantly across the flight envelope. To deal with this, the controller solves a nonlinear optimisation problem to compute the required attitude and thrust. A novel approach to control allocation based on dynamic computation of input effectiveness matrices was develop by Auterion [7], which was shown to allow a single form of control allocation for hybrid UAV, instead of different control allocation schemes for each flight mode. The performance was demonstrated with an *E-Flite Convergence VTOL*, Fig. 1, which was able to fly in an intermediate configuration. There were still limitations since the effectiveness matrix calculation was done by linearising the input influence on the dynamics around a constant trim point. As such, the UAV cannot fly in cruise flight and there are constraints on the tilt angles due to the linearisation not being valid in every flight configuration. Nonetheless, it is a considerable step towards a unified control structure for tiltrotor UAV.

3 Modelling

This section presents the modelling concepts used in this work. The model is based on the *E-Flite Convergence VTOL*.

We define an inertial frame of reference $\{\mathcal{I}\} = \{O_\mathcal{I};\ \hat{\boldsymbol{\imath}}_\mathcal{I},\ \hat{\boldsymbol{\jmath}}_\mathcal{I},\ \hat{\boldsymbol{k}}_\mathcal{I}\}$, which will be a local NED frame, and a body frame $\{\mathcal{B}\} = \{O_\mathcal{B};\ \hat{\boldsymbol{\imath}}_\mathcal{B},\ \hat{\boldsymbol{\jmath}}_\mathcal{B},\ \hat{\boldsymbol{k}}_\mathcal{B}\}$ [8]. Frame $\{\mathcal{B}\}$ is defined by having its origin $O_\mathcal{B}$ on the UAV's centre of mass (CoM), the x-axis $\hat{\boldsymbol{\imath}}_\mathcal{B}$ pointing forward, the y-axis $\hat{\boldsymbol{\jmath}}_\mathcal{B}$ pointing to the right, and the z-axis $\hat{\boldsymbol{k}}_\mathcal{B}$ pointing downward. The UAV has two tilting rotors that tilt longitudinally in a pitching motion. Following the approach in [9], two more coordinate frames $\{\mathcal{T}_1\}$ and $\{\mathcal{T}_2\}$ are introduced, for the right and left rotors, respectively. The positions of the origins of $\{\mathcal{T}_1\}$ and $\{\mathcal{T}_2\}$, with respect to $\{\mathcal{B}\}$, are $\mathbf{r}_1 = \begin{bmatrix} r_{1,x} & r_{1,y} & r_{1,z} \end{bmatrix}^\mathsf{T}$and $\mathbf{r}_2 = \begin{bmatrix} r_{2,x} & r_{2,y} & r_{2,z} \end{bmatrix}^\mathsf{T}$, respectively. These frames are represented graphically in Fig. 1. Let γ_1 and γ_2 denote the right and left rotors' tilt angles, respectively. The orientation of $\{\mathcal{T}_i\}$, $i = \{1, 2\}$, relative to $\{\mathcal{B}\}$is given by the rotation matrix

$$
{}^{\mathcal{B}}_{\mathcal{T}_i}\mathbf{R}(\gamma_i) = \begin{bmatrix} \cos(\gamma_i) & 0 & \sin(\gamma_i) \\ 0 & 1 & 0 \\ -\sin(\gamma_i) & 0 & \cos(\gamma_i) \end{bmatrix} \tag{1}
$$

3.1 Aerodynamic Forces and Moments

Aerodynamic phenomena are significant for hybrid UAVs. The aerodynamic forces, $\mathbf{F}_{\text{aero}}$, and moments, $\mathbf{M}_{\text{aero}}$, are divided into two categories: longitudinal and lateral. The model follows [8], with some adaptations.

We start by considering the lift force, $\mathbf{F}_{\text{Lift}}$, and drag force, $\mathbf{F}_{\text{Drag}}$, with magnitudes given by

$$F_{\text{Lift}} = \frac{1}{2}\rho S(C_{\text{L}}(\alpha) + (1-\sigma(\alpha))C_{\text{L},\delta_{\text{e}}}\delta_{\text{e}})\|^{\mathcal{B}}\mathbf{v}\|^2, \tag{2}$$

$$F_{\text{Drag}} = \frac{1}{2}\rho S(C_{\text{D}}(\alpha) + (1-\sigma(\alpha))C_{\text{D},\delta_{\text{e}}}\delta_{\text{e}})\|^{\mathcal{B}}\mathbf{v}\|^2, \tag{3}$$

with air density ρ, wing surface area S, body velocity ${}^{\mathcal{B}}\mathbf{v} = \begin{bmatrix} u & v & w \end{bmatrix}^{\mathsf{T}}$, lift and drag coefficients $C_{\text{L}}(\alpha)$ and $C_{\text{D}}(\alpha)$, angle of attack $\alpha = \text{atan2}(w, u)$, lift and drag coefficients $C_{\text{L},\delta_{\text{e}}}$ and $C_{\text{D},\delta_{\text{e}}}$ related to the elevator angle δ_{e}. Function $\sigma(\alpha)$ is a sigmoid function of the angle of attack. The elevator angle δ_{e} is given by $\delta_{\text{e}} = \delta_{\text{e,r}} + \delta_{\text{e,l}}$, with $\delta_{\text{e,r}}$ and $\delta_{\text{e,l}}$ the right and left elevon angles.. The lift and drag coefficients are given by

$$C_{\text{L}}(\alpha) = (1-\sigma(\alpha))\left(C_{\text{L},0} + C_{\text{L},\alpha}\ \alpha\right) + \sigma(\alpha)\left(2\,\text{sign}(\alpha)\ \sin^2(\alpha)\ \cos(\alpha)\right), \tag{4}$$

$$C_{\text{D}}(\alpha) = C_{\text{parasitic}} + \frac{(C_{\text{L},0} + C_{\text{L},\alpha}\,\alpha)^2}{(\pi\, e_{\text{Osw}}\ AR)}, \tag{5}$$

with $C_{\text{L},0}$ being the value of the lift coefficient when $\alpha = 0$, $C_{\text{L},\alpha}$ the coefficient of a linear term, $C_{\text{parasitic}}$ a coefficient related to parasitic drag, e_{Osw} the Oswald efficiency factor, and AR the UAV aspect ratio. The function $\sigma(\alpha)$ is a sigmoid function. It is mostly used as a weight, so as to give more importance to aerodynamic phenomena when the angle of attack is small and less importance otherwise, since when the UAV flies in rotary-wing mode, aerodynamics do not have as great an influence as in fixed-wing mode.

The longitudinal force components $F_{\text{aero},i}$ and $F_{\text{aero},k}$ are given by

$$\begin{bmatrix} F_{\text{aero},i} \\ F_{\text{aero},k} \end{bmatrix} = \begin{bmatrix} \cos(\alpha) & -\sin(\alpha) \\ \sin(\alpha) & \cos(\alpha) \end{bmatrix} \begin{bmatrix} -F_{\text{Drag}} \\ -F_{\text{Lift}} \end{bmatrix}. \tag{6}$$

In addition, there is also a pitching moment $M_{\text{aero},j}$ to be considered, given by

$$M_{\text{aero},j} = \frac{\rho S c}{2}(1-\sigma(\alpha))\left(C_{\text{m}_0} + C_{\text{m}_\alpha}\alpha + C_{\text{m}_{\text{e}}}\delta_{\text{e}}\right)\|^{\mathcal{B}}\mathbf{v}\|^2, \tag{7}$$

with wing mean chord c, pitch coefficient C_{m_0} when $\alpha = 0$ and $\delta_{\text{e}} = 0$, and pitch static stability coefficient C_{m_α}.

The lateral force component $F_{\text{aero},j}$, the roll $M_{\text{aero},i}$ and the yaw $M_{\text{aero},k}$ components of $\mathbf{F}_{\text{aero}}$ and $\mathbf{M}_{\text{aero}}$ are given by

$$F_{\text{aero},j} = \frac{1}{2}\rho S(1-\sigma(\alpha))\left(C_{\text{Y}_\beta}\beta + C_{\text{Y}_{\text{a}}}\delta_{\text{a}}\right)\|^{\mathcal{B}}\mathbf{v}\|^2, \tag{8}$$

$$M_{\text{aero},i} = \frac{1}{2}\rho S b(1-\sigma(\alpha))\left(C_{\text{l}_\beta}\beta + C_{\text{l}_{\text{a}}}\delta_{\text{a}}\right)\|^{\mathcal{B}}\mathbf{v}\|^2, \tag{9}$$

$$M_{\text{aero},k} = \frac{1}{2}\rho S b(1-\sigma(\alpha))\left(C_{\text{n}_\beta}\beta + C_{\text{n}_{\text{a}}}\delta_{\text{a}}\right)\|^{\mathcal{B}}\mathbf{v}\|^2, \tag{10}$$

with sideslip angle β , wingspan b, lateral force coefficient concerning β and δ_{a}, C_{Y_β} and $C_{\text{Y}_{\text{a}}}$, respectively, roll and yaw static stability coefficients, C_{l_β} and C_{n_β}, deflection control coefficient concerning roll $C_{\text{l}_{\text{a}}}$, deflection cross-control coefficient concerning yaw $C_{\text{n}_{\text{a}}}$, and aileron deflection angle $\delta_{\text{a}} = -\delta_{\text{e,r}} + \delta_{\text{e,l}}$.

3.2 Rotor Forces and Moments

The UAV has two front tilting rotors, one on each wing, and one fixed rotor on its tail. Denoting the right and left rotors by rotor $i = \{1,\ 2\}$, respectively, each spins with angular velocity ω_i, with rotor 1 spinning anticlockwise and rotor 2 clockwise, and generates a force $\mathbf{F}_i$ and a moment $\mathbf{M}_i$, with magnitudes given by $F_i = k_{\mathrm{F}}\omega_i^2 \frac{1}{2}\rho\, S_{\mathrm{rotor}} \|\mathbf{v}_{\mathrm{air,rotor}}\|^2$and $M_i = k_{\mathrm{M}}\omega_i^2$, with k_{F} and k_{M} force and moment coefficients related to these rotors, S_{rotor} the rotor surface area, and $\mathbf{v}_{\mathrm{air,rotor}}$ the velocity of the air going into the rotor. Force $\mathbf{F}_i$ is applied in the direction of $\hat{\boldsymbol{\imath}}_{\mathcal{T}_i}$, and the moment $\mathbf{M}_i$ is applied about the axis $\hat{\boldsymbol{\imath}}_{\mathcal{T}_i}$, with opposite signal relative to the angular velocity ω_i. The overall force $\mathbf{F}_{\mathrm{wr}}$ and moment $\mathbf{M}_{\mathrm{wr}}$ from the front rotors acting on the CoM is given by

$$\mathbf{F}_{\mathrm{wr}} = \begin{bmatrix} F_1\ \cos(\gamma_1) + F_2\ \cos(\gamma_2) \\ 0 \\ -F_1 \sin(\gamma_1) - F_2 \sin(\gamma_2) \end{bmatrix} \qquad \mathbf{M}_{\mathrm{wr}} = \begin{bmatrix} M_1\ \cos(\gamma_1) - M_2\ \cos(\gamma_2) \\ 0 \\ -M_1 \sin(\gamma_2) + M_2 \sin(\gamma_2) \end{bmatrix} \tag{11}$$

Forces $\mathbf{F}_1$ and $\mathbf{F}_2$, applied at $\mathbf{r}_1$ and $\mathbf{r}_2$, generate moment $\mathbf{M}_{\mathrm{F,wr}}$, given by

$$\mathbf{M}_{\mathrm{F,wr}} = \mathbf{r}_1 \times \left({}^{\mathcal{B}}_{\mathcal{T}_1}\mathbf{R}\ \mathbf{F}_1\right) + \mathbf{r}_2 \times \left({}^{\mathcal{B}}_{\mathcal{T}_2}\mathbf{R}\ \mathbf{F}_2\right) \tag{12}$$

There is also the force $\mathbf{F}_{\mathrm{tr}}$ and a moment $\mathbf{M}_{\mathrm{tr}}$ from the tail rotor, which spins anticlockwise with angular velocity ω_{tr}, given by $\mathbf{F}_{\mathrm{tr}} = -F_{\mathrm{tr}}\,\hat{\boldsymbol{k}}_{\mathcal{B}}$ and $\mathbf{M}_{\mathrm{tr}} = M_{\mathrm{tr}}\,\hat{\boldsymbol{k}}_{\mathcal{B}}$. The magnitudes are given by $F_{\mathrm{tr}} = k_{\mathrm{F,tr}}\omega_{\mathrm{tr}}^2$ and $M_{\mathrm{tr}} = k_{\mathrm{M,tr}}\omega_{\mathrm{tr}}^2$, with $k_{\mathrm{F,tr}}$ and $k_{\mathrm{M,tr}}$ the force and moment coefficients for the tail rotor. Since $\mathbf{F}_{\mathrm{tr}}$ is not applied directly to the CoM, it generates a pitching moment $\mathbf{M}_{\mathrm{F,tr}}$. Consider the position vector $\mathbf{r}_{\mathrm{tr}}$ with origin in the CoM with magnitude equal to the distance between the CoM and the point where $\mathbf{F}_{\mathrm{tr}}$ is applied, and pointing to said point. Then, the moment $\mathbf{M}_{\mathrm{F,tr}}$ is $\mathbf{M}_{\mathrm{F,tr}} = \mathbf{r}_{\mathrm{tr}} \times \mathbf{F}_{\mathrm{tr}}$, which, assuming that the angle between the position and force vectors $\angle(\mathbf{r}_{\mathrm{tr}},\ \mathbf{F}_{\mathrm{tr}}) \approx \frac{\pi}{2}$, then $\mathbf{M}_{\mathrm{F,tr}} = -\|\mathbf{r}_{tr}\|\ k_{\mathrm{F,tr}}\ \omega_{\mathrm{tr}}^2\ \hat{\boldsymbol{\jmath}}_{\mathcal{B}}$.

Combining the above expressions, the total force $\mathbf{F}_{\mathrm{rotors}}$ and moment $\mathbf{M}_{\mathrm{rotors}}$ generated by the rotors are

$$\mathbf{F}_{\mathrm{rotors}} = \mathbf{F}_{\mathrm{wr}} + \mathbf{F}_{\mathrm{tr}}\,, \qquad \mathbf{M}_{\mathrm{rotors}} = \mathbf{M}_{\mathrm{wr}} + \mathbf{M}_{\mathrm{tr}} + \mathbf{M}_{\mathrm{F,wr}} + \mathbf{M}_{\mathrm{F,tr}}\,. \tag{13}$$

3.3 Kinematic and Dynamic Equations

Let the position of the CoM w.r.t. $\{\mathcal{I}\}$ be denoted by $\mathbf{p}$, and the linear velocity of frame $\{\mathcal{B}\}$ relative to $\{\mathcal{I}\}$, expressed in $\{\mathcal{I}\}$, by $\mathbf{v}$. Further, let $\boldsymbol{q} = (q_0,\ q_1,\ q_2,\ q_3) = (q_0,\ \mathbf{q})$ be the quaternion that represents the UAV's orientation and $\boldsymbol{\omega}$ the UAV's angular velocity. The kinematic equations of motion are

$$\dot{\mathbf{p}} = \mathbf{v}\,, \qquad \dot{\boldsymbol{q}} = \frac{1}{2}\,\mathbf{S}_{\mathrm{q}}(\boldsymbol{q})\,\boldsymbol{\omega}\ . \tag{14}$$

In addition, acting on the UAV are the force due to gravity $\mathbf{F}_{\mathrm{g}}$, the aerodynamic forces and moments, $\mathbf{F}_{\mathrm{aero}}$ and $\mathbf{M}_{\mathrm{aero}}$, and rotor forces and moments, $\mathbf{F}_{\mathrm{rotors}}$ and $\mathbf{M}_{\mathrm{rotors}}$. Hence, the Newton-Euler equations of motion are

$$m\dot{\mathbf{v}} = \mathbf{F}_{\mathrm{g}} + {}^{\mathcal{I}}_{\mathcal{B}}\mathbf{R}\,(\mathbf{F}_{\mathrm{aero}} + \mathbf{F}_{\mathrm{rotors}})\ , \tag{15}$$

$$\mathbf{J}\,\dot{\boldsymbol{\omega}} = -\mathbf{S}(\boldsymbol{\omega})\,\mathbf{J}\,\boldsymbol{\omega} + \mathbf{M}_{\mathrm{aero}} + \mathbf{M}_{\mathrm{rotors}}\ , \tag{16}$$

with m and $\mathbf{J}$ being the mass and inertia matrix of the UAV, respectively, and ${}^{\mathcal{I}}_{\mathcal{B}}\mathbf{R}$ the rotation matrix from $\{\mathcal{B}\}$ to the $\{\mathcal{I}\}$. In the absence of wind, the aerodynamic force and moment, as well as the rotors force and moment, may be decomposed into forces and moments that depend solely on the state (more precisely the velocity) of the UAV, $\mathbf{F}_{\text{state}}(\mathbf{v})$ and $\mathbf{M}_{\text{state}}(\mathbf{v})$, and on the states and inputs, $\mathbf{F}_{\text{inputs}}(\mathbf{v}, \mathbf{u})$ and $\mathbf{M}_{\text{inputs}}(\mathbf{v}, \mathbf{u})$, with inputs $\mathbf{u} = \begin{bmatrix}\omega_1 & \omega_2 & \omega_{\text{tr}} & \gamma_1 & \gamma_2 & \delta_{\text{e,l}} & \delta_{\text{e,r}}\end{bmatrix}$, meaning $\mathbf{F}_{\text{aero}}+\mathbf{F}_{\text{rotors}} = \mathbf{F}_{\text{state}}+\mathbf{F}_{\text{inputs}}$ and $\mathbf{M}_{\text{aero}}+\mathbf{M}_{\text{rotors}} = \mathbf{M}_{\text{state}}+\mathbf{M}_{\text{inputs}}$. This rearrangement will be useful for the control strategy in Section 4. The system error dynamics will also be of importance. The position error $\widetilde{\mathbf{p}}$ is defined as the difference between the position and its reference and the velocity error $\widetilde{\mathbf{v}}$ as the difference between the velocity and its reference, i.e.

$$\widetilde{\mathbf{p}} = \mathbf{p} - \mathbf{p}_{\text{ref}} \,, \qquad \widetilde{\mathbf{v}} = \dot{\widetilde{\mathbf{p}}} = \mathbf{v} - \mathbf{v}_{\text{ref}} \,. \tag{17}$$

The time-derivative of the velocity error is thus given by

$$\dot{\widetilde{\mathbf{v}}} = \mathbf{g} + \frac{1}{m}\,{}^{\mathcal{I}}_{\mathcal{B}}\mathbf{R}\,\mathbf{F}_{\text{states}} + \frac{1}{m}\,{}^{\mathcal{I}}_{\mathcal{B}}\mathbf{R}\,\mathbf{F}_{\text{inputs}} - \mathbf{a}_{\text{ref}} \tag{18}$$

Regarding attitude, the orientation error $\widetilde{\boldsymbol{q}}$, defined as the quaternion product of the orientation reference conjugate by the orientation of the UAV, with a corresponding error rotation matrix $\widetilde{\mathbf{R}}$, and the angular velocity error $\widetilde{\boldsymbol{\omega}}$ are given by

$$\widetilde{\boldsymbol{q}} = (\widetilde{q}_0, \widetilde{\mathbf{q}}) = \bar{\boldsymbol{q}}_{\text{ref}} \circ \boldsymbol{q} \,, \quad \widetilde{\mathbf{R}} = \mathbf{R}(\widetilde{\boldsymbol{q}}) \,, \quad \widetilde{\boldsymbol{\omega}} = \boldsymbol{\omega} - \widetilde{\mathbf{R}}\,\boldsymbol{\omega}_{\text{ref}} \,. \tag{19}$$

The time-derivative of $\widetilde{\boldsymbol{\omega}}$, the angular acceleration error, is given by

$$\dot{\widetilde{\boldsymbol{\omega}}} = \mathbf{J}^{-1}\left(-\mathbf{S}(\boldsymbol{\omega})\,\mathbf{J}\,\boldsymbol{\omega} + \mathbf{M}_{\text{states}} + \mathbf{M}_{\text{inputs}}\right) - \left(\widetilde{\mathbf{R}}\,\dot{\boldsymbol{\omega}}_{\text{ref}} - \mathbf{S}(\widetilde{\boldsymbol{\omega}})\,\widetilde{\mathbf{R}}\,\boldsymbol{\omega}_{\text{ref}}\right) \,. \tag{20}$$

4 Control

The overall control system architecture is shown in Figure 2. The Trajectory Handler provides the trajectory references ($\mathbf{p}_{\text{ref}}$, $\mathbf{v}_{\text{ref}}$, $\mathbf{a}_{\text{ref}}$) to the Controller, which calculates the reference force $\mathbf{F}_{\text{ref}}$ and moment $\mathbf{M}_{\text{ref}}$. The Controller is divided into two blocks: the position controller and attitude controller. The position controller receives the trajectory reference and the UAV state and computes $\mathbf{F}_{\text{ref}}$, the orientation quaternion reference $\boldsymbol{q}_{\text{ref}}$, and the angular velocity reference $\boldsymbol{\omega}_{\text{ref}}$. The attitude controller receives $\boldsymbol{q}_{\text{ref}}$ and $\boldsymbol{\omega}_{\text{ref}}$ and calculates $\mathbf{M}_{\text{ref}}$. The Control Allocation block computes the input values $\mathbf{u}$ that generate $\mathbf{F}_{\text{ref}}$ and $\mathbf{M}_{\text{ref}}$, which are then fed into UAV model.

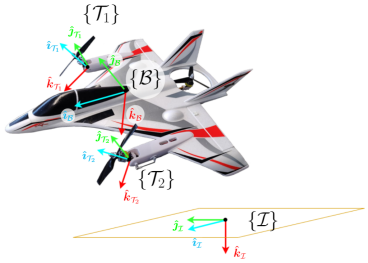

Fig. 1: Coordinate frames

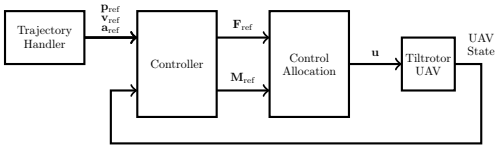

Fig. 2: Control System Architecture

4.1 Position and Attitude Control

Regarding the position control, the objective is to have the UAV closely follow the trajectory reference. To drive error dynamics related to linear motion to zero, we first define the system

$$\begin{aligned} \boldsymbol{\xi}_1 &= \tilde{\mathbf{p}}, \\ \boldsymbol{\xi}_2 &= \tilde{\mathbf{v}} - \boldsymbol{\alpha}_1(\boldsymbol{\xi}_1), \end{aligned} \tag{21}$$

with $\boldsymbol{\alpha}_1(\boldsymbol{\xi}_1)$being the virtual controller to be calculated. A candidate Lyapunov function is proposed, defined as

$$V_1 = \frac{1}{2}\,\boldsymbol{\xi}_1^{\mathsf{T}}\,\boldsymbol{\xi}_1 + \frac{k_{1,\mathrm{I}}}{2}\left[\int \boldsymbol{\xi}_1 dt\right]^{\mathsf{T}}\left[\int \boldsymbol{\xi}_1 dt\right] + \frac{1}{2}\,\boldsymbol{\xi}_2^{\mathsf{T}}\,\boldsymbol{\xi}_2\,. \tag{22}$$

This Lyapunov function is quadratic in the position error $\boldsymbol{\xi}_1$, in the integral of the position error, and in the velocity error $\boldsymbol{\xi}_2$. Taking the virtual controller to be $\boldsymbol{\alpha}_1(\boldsymbol{\xi}_1) = -k_1\,\boldsymbol{\xi}_1 - k_{1,\mathrm{I}}\left[\int \boldsymbol{\xi}_1 dt\right]$ with constants $k_1 > 0$ and $k_{1,\mathrm{I}} > 0$, and defining $\mathbf{F}_{\mathrm{ref}}$ as the $\mathbf{F}_{\mathrm{input}}$ that stabilises the system, if

$$\mathbf{F}_{\mathrm{ref}} = \text{-}\mathbf{F}_{\mathrm{g}} \text{ - } \mathbf{F}_{\mathrm{state}} + m\left[\mathbf{a}_{\mathrm{ref}} \text{ - } (k_1 + k_2)\tilde{\mathbf{v}} \text{ - } (1 + k_{1,\mathrm{I}} + k_1 k_2)\tilde{\mathbf{p}} \text{ - } k_{1,\mathrm{I}} k_2 \int \tilde{\mathbf{p}}\, dt\right] \tag{23}$$

with $k_2 > 0$, then $\dot{V}_1 = -k_1\,\|\,\boldsymbol{\xi}_1\|^2 - k_2\,\|\,\boldsymbol{\xi}_2\|^2 \leq 0$. Thus, with force reference $\mathbf{F}_{\mathrm{ref}}$, the position and velocity errors converge to $\mathbf{0}$.

Calculating the orientation reference for tiltrotor UAVs is not as straightforward as for UAVs with fixed rotors. The approach taken involves an optimisation problem, similar to [6]. The main difficulty stems from the additional degree of freedom that the tilting rotors provide. First, we find an estimate of the tilt angles, fixing the generated force from the front rotors in a certain direction. This does not solve the problem completely, but simplifies it. We assume that the estimated tilt angle is the same for both rotors and that the resulting pitching moment should be zero. The tilt angle estimate γ_{est} is given by

$$\gamma_{\mathrm{est}} = \mathrm{sat}\left(\mathrm{atan2}\left(F_{\mathrm{ref},k}\ ,\ F_{\mathrm{ref},i}\left(1 + \frac{r_{1,i}}{r_{\mathrm{tr},i}}\right)\right)\right)\ , \tag{24}$$

which is limited between the maximum and minimum values of the tilt angle. Since the rotors tilt in a pitching motion, the pitch of the UAV influences γ_{est}, but in normal conditions, tiltrotor aircraft are characterised by a small pitch angle in any flight mode. Despite simplifying the attitude reference calculation by setting a tilt angle estimate, it is still complex. To determine the attitude, the problem is formulated as the following optimisation problem:

$$\min_{\phi,\,\theta,\,\psi,F_1,\,F_2,\,F_{\mathrm{tr}}} \left\|{}^{\mathcal{I}}_{\mathcal{B}}\mathbf{R}(\phi,\,\theta,\,\psi)\ \mathbf{F}_{\mathrm{rotors}} - \mathbf{F}_{\mathrm{ref}}\right\|_2 \tag{25}$$

$$\begin{aligned} \text{subject to} \quad & 0 \leq F_1\,,\ 0 \leq F_2\,,\ 0 \leq F_{\mathrm{tr}} \\ & -\tfrac{\pi}{2} \leq \phi \leq \tfrac{\pi}{2}\,,\ \theta_{\min} \leq \theta \leq \theta_{\max}\,,\ -\pi \leq \psi \leq \pi \end{aligned}$$

The variables are the roll, pitch and yaw angles, and the forces generated by each rotor, encoded in $\mathbf{F}_{\mathrm{rotors}}$. The objective is to minimise the difference between the reference force and the force generated by rotors in a desired attitude encoded by

${}^{\mathcal{I}}_{\mathcal{B}}\mathbf{R}$. The interference between the aircraft's pitch and tilt angles is addressed by limiting the pitch to $[\theta_{\min}, \theta_{\max}]$. From ${}^{\mathcal{I}}_{\mathcal{B}}\mathbf{R}_{\text{ref}}$, the reference quaternion $\boldsymbol{q}_{\text{ref}}$ can be calculated, followed by the angular velocity reference $\boldsymbol{\omega}_{\text{ref}} = k_\omega \text{ vec}\,(\boldsymbol{q}_{\text{ref}} \circ \boldsymbol{q})$, with $k_\omega > 0$ is a constant and vec$(\cdot)$ returns the vector part of a quaternion. Making use of the error dynamics model, we define the system

$$\begin{aligned} \boldsymbol{\xi}_3 &= \widetilde{\mathbf{q}}, \\ \boldsymbol{\xi}_4 &= \widetilde{\boldsymbol{\omega}} - \boldsymbol{\alpha}_2(\boldsymbol{\xi}_3), \end{aligned} \tag{26}$$

with virtual controller $\boldsymbol{\alpha}_2(\boldsymbol{\xi}_3)$. We propose a candidate Lyapunov function V_2, defined as

$$V_2 = \frac{1}{2}\, \boldsymbol{\xi}_3^{\mathsf{T}}\, \boldsymbol{\xi}_3 + \frac{1}{2}\, \boldsymbol{\xi}_4^{\mathsf{T}}\, \boldsymbol{\xi}_4\,. \tag{27}$$

This Lyapunov function is quadratic in the orientation error $\boldsymbol{\xi}_3$ and the angular velocity error $\boldsymbol{\xi}_4$. Let us denote $\widetilde{\mathbf{Q}} = \mathbf{S}(\boldsymbol{\xi}_3) + \sqrt{1 - \boldsymbol{\xi}_3^{\mathsf{T}}\boldsymbol{\xi}_3}\, \mathbf{I}_{3\times 3}$ and define the virtual controller as $\boldsymbol{\alpha}_2(\boldsymbol{\xi}_3) = -2k_3\widetilde{\mathbf{Q}}^{-1}\boldsymbol{\xi}_3$, with constant $k_3 > 0$. Defining $\mathbf{M}_{\text{ref}}$ as the $\mathbf{M}_{\text{input}}$ that accomplishes this, the expression is given by

$$\mathbf{M}_{\text{ref}} = \mathbf{S}(\boldsymbol{\omega})\mathbf{J}\boldsymbol{\omega} \text{ - } \mathbf{M}_{\text{state}} + \mathbf{J}\left(\widetilde{\mathbf{R}}\dot{\boldsymbol{\omega}}_{\text{ref}} \text{ - } \mathbf{S}(\boldsymbol{\omega})\widetilde{\mathbf{R}}\boldsymbol{\omega}_{\text{ref}} + \dot{\boldsymbol{\alpha}}_2(\boldsymbol{\xi}_3) \text{ - } k_4\boldsymbol{\xi}_4 \text{ - } \frac{1}{2}\widetilde{\mathbf{Q}}^{\mathsf{T}}\boldsymbol{\xi}_3\right), \tag{28}$$

where $k_4 > 0$ is a constant. With $\mathbf{M}_{\text{ref}}$, $\dot{V}_2 = -k_3 \parallel \boldsymbol{\xi}_3\parallel^2 - k_4 \parallel \boldsymbol{\xi}_4\parallel^2 \leq 0$, and the orientation and angular velocity errors converge to $\mathbf{0}$.

4.2 Control Allocation

The control allocation issue is complex, particularly considering a unified control approach. As the system is considered as a whole, depending on the state of the UAV at each instant, the control allocation strategy should be able to calculate the necessary inputs without *a priori* information of the functioning configuration. The reference trajectories, which will be described in Section 5, deal mostly with longitudinal motion, so longitudinal motion will be given more significance than lateral motion in this allocation scheme. The longitudinal forces and moment depend nonlinearly on $\mathbf{u}_{\text{long}} = \{\omega_1, \omega_2, \omega_{\text{tr}}, \gamma_1, \gamma_2, \delta_{\text{e}}\}$. To allocate these forces and moment, the following optimisation problem is formulated:

$$\underset{\mathbf{u}_{\text{long}}}{\text{minimise}} \quad \left\| \begin{bmatrix} F_{\text{ref,i}} \\ F_{\text{ref,k}} \\ M_{\text{ref,j}} \end{bmatrix} - \begin{bmatrix} F_{\text{input,i}}(\mathbf{u}_{\text{long}}) \\ F_{\text{input,k}}(\mathbf{u}_{\text{long}}) \\ M_{\text{input,j}}(\mathbf{u}_{\text{long}}) \end{bmatrix} \right\|_2 , \tag{29}$$

$$\text{subject to } \mathbf{u}_{\text{long,min}} \leq \mathbf{u}_{\text{long}} \leq \mathbf{u}_{\text{long,max}}$$

which is solved at each time instant by a nonlinear optimisation solver.

The lateral aerodynamic force and moments depend linearly on δ_{a}. Lateral motion can be achieved via differential thrust of the front rotors, depending on the direction given by the tilt angle. Considering the trajectories at hand and to simplify the problem, an equal tilt angle γ is assumed, given by the average of the angles calculated in (29), making the lateral moments related to the rotors

dependent on $\omega_{\mathrm{d}} = (\omega_1^2 - \omega_2^2)$. The allocation problem is formulated as the following constrained least squares problem:

$$\underset{\omega_{\mathrm{d}},\delta_{\mathrm{a}}}{\text{minimise}} \left\| \begin{bmatrix} 0 & 0.5\rho S(1-\sigma(\alpha))C_{\mathrm{Y_a}} \\ -r_{1,\mathrm{y}}k_{\mathrm{F}}\sin(\gamma) & 0.5\rho Sb(1-\sigma(\alpha))C_{\mathrm{l_a}} \\ -r_{1,\mathrm{y}}k_{\mathrm{F}}\cos(\gamma) & 0.5\rho Sb(1-\sigma(\alpha))C_{\mathrm{n_a}} \end{bmatrix} \begin{bmatrix} \omega_{\mathrm{d}} \\ \delta_{\mathrm{a}} \end{bmatrix} - \begin{bmatrix} F_{\mathrm{ref,j}} \\ M_{\mathrm{ref,i}} \\ M_{\mathrm{ref,k}} \end{bmatrix} \right\|_2^2 \tag{30}$$

$$\text{subject to} \quad \delta_{\mathrm{a,min}} \leq \delta_{\mathrm{a}} \leq \delta_{\mathrm{a,max}} \,.$$

4.3 Limitations

This control allocation approach presents limitations. Concerning the attitude reference, the pitch angle influences γ_{est}, which is addressed by assuming the pitch angle is always constrained between $\theta_{\min}$ and $\theta_{\max}$. This may not hold at all times and could jeopardise the computation. Formulating the attitude reference generation and the control allocation as a nonlinear optimisation problems creates further issues. The solver may take excessive time to solve the problem or fail to find a solution, and results may vary depending on the solver used. In the control allocation, the division into longitudinal and lateral dynamics, made to reduce the complexity, gives more significance to the longitudinal dynamics, at the expense of the lateral dynamics. An approach that takes into account both simultaneously and has a closed-form solution would be preferable, though such is difficult to obtain without some trade-off.

5 Simulation

The UAV is set to initially be at rest, in the origin of $\{\mathcal{I}\}$, and with $\{\mathcal{B}\}$ aligned with $\{\mathcal{I}\}$. The simulations were performed using Matlab and Simulink.

The reference trajectories, denoted by Traj. A and Traj. B, are simply the concatenation of a vertical and a horizontal segment. Both trajectories share the same upward segment, which presents a trapezoidal velocity profile, with initial position $\mathbf{p}_{\mathrm{i}} = \begin{bmatrix} 0 & 0 & 0 \end{bmatrix}$ and final $\mathbf{p}_{\mathrm{h}} = \begin{bmatrix} 0 & 0 & -2 \end{bmatrix}$ m. In Traj. A, the forward velocity is the UAV's trim velocity, $v_{\mathrm{for}} = 35.75\,\mathrm{m/s}$, and in Traj. B, the forward velocity is lower than trim, $v_{\mathrm{for}} = 25\,\mathrm{m/s}$. The upward segment takes place in $t = [0,\, 12]\,\mathrm{s}$, followed by the forward segment from then on. The plots are truncated at $t = 24\,\mathrm{s}$.

Fig. 3 and 4 show the plots of the reference and actual position for Traj. A and B, respectively. In both cases, the UAV follows the reference.

The forces and moments allocated by the control allocation scheme and generated by the actuators, w.r.t. $\{\mathcal{B}\}$, are shown in Fig. 5 to 8. As the UAV starts moving forward, there is a sharp increase in the forward force reference, which keeps increasing until the UAV stops accelerating. The vertical reference decreases in magnitude as the UAV moves forward and more lift is generated. In the final part of Traj. A, the forward force is $\approx 39.8\,\mathrm{N}$ and the vertical force is $-7.5\,\mathrm{N}$. In the corresponding part of Traj. B, the forward force is $\approx 23.3\,\mathrm{N}$ and

the vertical force is $-70.4\,\mathrm{N}$, but present small magnitude irregularities. Examining the moments, since the attitude only changes in terms of the pitch angle, it is natural that only the pitching moment reference changes. For Traj. A, in forward flight, the pitching moment reference stabilises at $\approx 2\,\mathrm{Nm}$ and during the acceleration part it presents two brief spikes of $\approx -5\,\mathrm{Nm}$, caused by starting and stopping accelerating and by the reduction of the tail rotor spin at $t = 15.5\,\mathrm{s}$. For Traj. B, the pitching moment exhibits irregular behaviour, contrasting with the results of the UAV in trim flight. Nonetheless, the control allocation scheme is able to allocate the references through the trajectory.

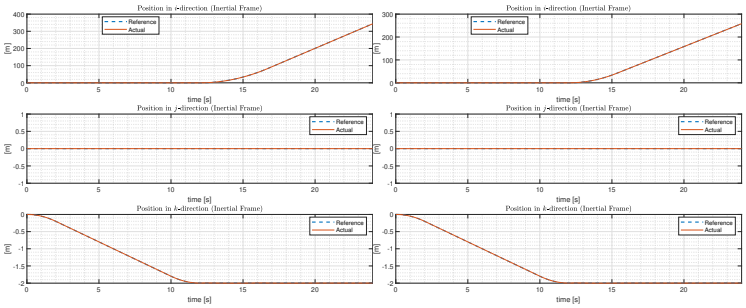

Fig. 3: Traj. A: Position

Fig. 4: Traj. B: Position

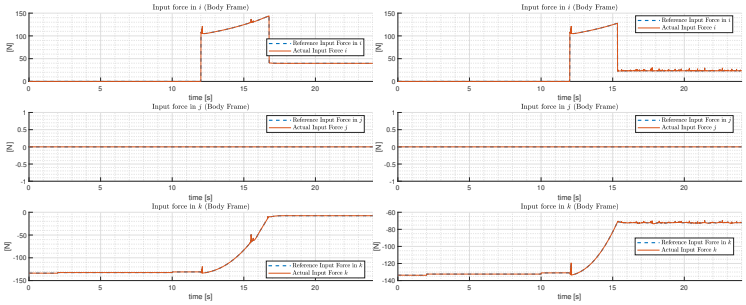

Fig. 5: Traj. A: Force in body

Fig. 6: Traj. B: Force in body

Considering the rotors' angular velocities as well as the tilt and elevon angles, in both trajectories, Fig. 9 to 12, the behaviour during the first segment of each trajectory is the same, with elevons fixed at zero deflection and rotors tilted upwards. As the UAV accelerates forward, the front rotors tilt forward and spin faster, the tail rotor initially speeds up to compensate the pitching moment but then slows down, and the elevons deflect upwards. For Traj. A, in constant velocity forward flight, the front rotors are fully tilted forward and spinning at $13.6\,\mathrm{rad/s}$, the tail rotor stops, and the elevons stabilise at $-0.02\,\mathrm{rad}$. For Traj. B, the front rotors are tilted at $\approx 28.6°$ (with brief small magnitude spikes) and spinning at $8.8\,\mathrm{rad/s}$, the tail rotor at $4.6\,\mathrm{rad/s}$ with some irregularities, and the elevons at $\approx -0.2\,\mathrm{rad}$ also with short small magnitude spikes.

Taking everything into account, the UAV is able to follow the trajectories, keeping a levelled attitude throughout, and the required forces and moments are

allocated. Moreover, in the forward flight part of Traj. A, the UAV is operating as a fixed-wing aircraft, and in Traj. B, the UAV stays in an intermediate state, with the front rotors tilted at an angle and the tail rotor still providing lift.

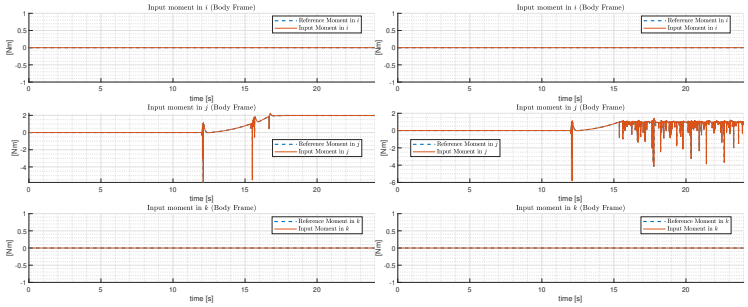

Fig. 7: Traj. A: Moment in body

Fig. 8: Traj. B: Moment in body

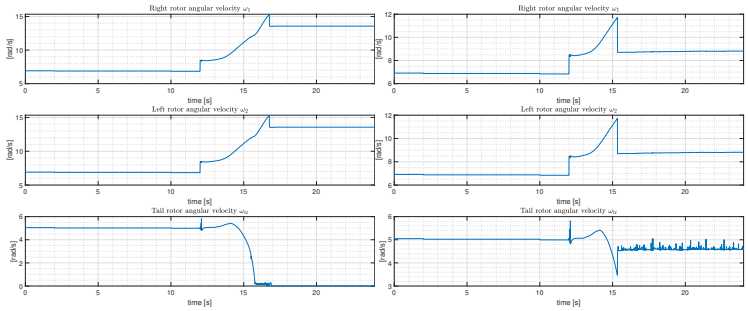

Fig. 9: Traj. A: Rotors' angular velocities

Fig. 10: Traj. B: Rotors' angular velocities

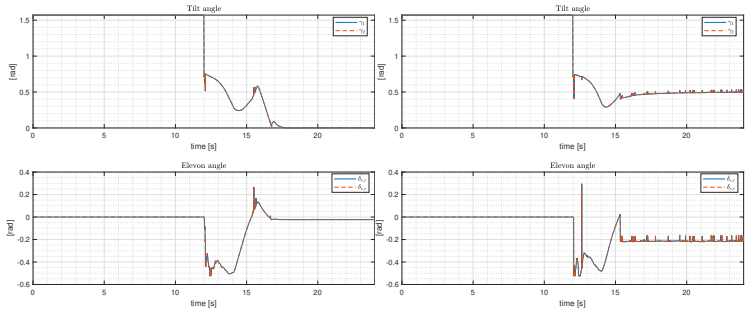

Fig. 11: Traj. A: Tilt and Elevon angles

Fig. 12: Traj. B: Tilt and Elevon angles

6 Conclusions

The main objective of this work was to take the first steps in developing a unified control approach that could be used by tri-tilrotor UAVs for trajectory

tracking. First, a model of a tri-tilrotor was derived. Afterwards, the control system architecture was presented, with the description of the attitude and position controllers, which generate force and moment references via backstepping. These controllers guaranteed stability, provided that the force and moment references were correctly allocated. A control allocation scheme, which gave more importance to force and moment references related to longitudinal motion, due to the trajectories that would be considered, was proposed. These strategies presented some limitations, which were discussed. Then, two trajectories of interest were defined, which differed in the velocity of the forward motion segment, in order to observe if in the one the UAV would fully transition into a fixed-wing configuration and in the other it would fly in an intermediate configuration. To validate the proposed unified control approach, simulations were performed for the two trajectories. The UAV was able to follow the references and in the anticipated configurations. However, in the second trajectory, certain references, as well as the inputs, presented an irregular behaviour when compared to the first case.

Acknowledgements This work was partially funded by FCT project REPLACE (PTDC/EEIAUT/32107/2017) which includes Lisboa 2020 and PIDDAC funds, project CAPTURE (PTDC/EEI-AUT/1732/2020), and also projects CTS (UIDB/00066/2020) and LARSYS (UIDB/50009/2020)

References

1. Guerreiro, B.: REPLACE Project., http://replace.isr.tecnico.ulisboa.pt. Last accessed: 26 Feb 2022
2. Ta, D., Fantoni, I. & Lozano, R.: Modeling and control of a tilt tri-rotor airplane. *Proceedings Of The American Control Conference*. pp. 131-136 (2012)
3. Yu, L., Zhang, D., Zhang, J. & Pan, C.: Modeling and attitude control of a tilt tri-rotor UAV. *Chinese Control Conference, CCC*. pp. 1103-1108 (2017,9)
4. Yuksek, B., Vuruskan, A., Ozdemir, U., Yukselen, M. & Inalhan, G.: Transition Flight Modeling of a Fixed-Wing VTOL UAV. *Journal Of Intelligent And Robotic Systems: Theory And Applications*. pp. 83-105 (2016)
5. Hartmann, P., Meyer, C. & Moormann, D.: Unified velocity control and flight state transition of unmanned tilt-wing aircraft. *Journal Of Guidance, Control, And Dynamics*. pp. 1348-1359 (2017)
6. Zhou, J., Lyu, X., Li, Z., Shen, S. & Zhang, F.: A unified control method for quadrotor tail-sitter UAVs in all flight modes: Hover, transition, and level flight. *IEEE International Conference On Intelligent Robots And Systems*. pp. 4835-4841 (2017)
7. Lecoeur, J. & Fuhrer, S.: Control Allocation: reworking the PX4 mixing system — PX4 Developer Summit Virtual 2020, https://youtu.be/xjLM9whwjO4. Last accessed: 26 Feb 2022
8. Beard, R. & McLain, T.: Small unmanned aircraft: Theory and practice. *Small Unmanned Aircraft: Theory And Practice*. (2012)
9. Kendoul, F., Fantoni, I. & Lozano, R.: Modeling and control of a small autonomous aircraft having two tilting rotors. *Proceedings Of The 44th IEEE Conference On Decision And Control, And The European Control Conference, CDC-ECC '05*. pp. 8144-8149 (2005)